Organic & Biomolecular Chemistry

Accepted Manuscript

This article can be cited before page numbers have been issued, to do this please use: R. Shah, A. Zhou and C. R. Wagner, *Org. Biomol. Chem.*, 2017, DOI: 10.1039/C7OB02472J.

ROYAL SOCIETY OF CHEMISTRY

rsc.li/obc

DOI: 10.1039/C7OB02472J

Journal Name

ARTICLE

Switch-on Fluorescent/FRET Probes to Study Human Histidine Triad Nucleotide Binding Protein 1 (hHint1), a Novel Target for Opioid Tolerance and Neuropathic Pain

Rachit Shah,[a] Andrew Zhou[a] and Carston R. Wagner[a]

Received 00th January 20xx,
Accepted 00th January 20xx

DOI: 10.1039/x0xx00000x

www.rsc.org/

Histidine Triad Nucleotide Binding Protein 1 (Hint1) has emerged to be an important post-synaptic protein associated with a variety of central nervous system disorders such as pain, addiction, and schizophrenia. Recently, inhibition of histidine nucleotide binding protein 1 (Hint1) with a small nucleoside inhibitor has shown promise as a new therapeutic strategy for the treatment of neuropathic pain. Herein, we describe the first rationally designed small molecule switch-on probes with dual fluorescence and FRET properties to study Hint1. Two non-natural fluorescent nucleosides with a fluorescent lifetime of 20 and 25 ns were each coupled through a linker to the indole ring, i.e. probes **7** and **8**. Both probes were found to be water soluble and quenched intramolecularly via photoinduced electron transfer (PET) resulting in minimal background fluorescence. Upon incubating with Hint1 compound **7** and **8** exhibited a 40- and 16- fold increase in the fluorescence intensity compared to the control. Compounds **7** and **8** bind Hint1 with a dissociation constant of 0.121 ± 0.02 and 2.2 ± 0.36 µM, respectively. We demonstrate that probe **8** exhibits a switch-on FRET property with an active site tryptophan residue (W123). We show the utility of probes in performing quantitative ligand displacement studies, as well as in selective detection of Hint1 in the cell lysates. These probes should be useful for studying the dynamics of the active site, as well as for the development of fluorescence lifetime based high throughput screening assay to identify novel inhibitors for Hint1 in future.

Introduction

Histidine triad nucleotide binding protein 1 (Hint1) has emerged as a key regulator of pain, opioid tolerance and addiction properties in the central nervous system (CNS).[1-3] Hint1 belongs to the histidine triad (HIT) superfamily which are characterized by their conserved nucleotide binding motif, His-X-His-X-His-XX, where X is a hydrophobic residue. hHint1 exists as a homodimer and possesses nucleoside phosphoramidase and acyl-AMP hydrolase activity, with a preference for substrates with purine over pyrimidine nucleosides.[4, 5] The nucleoside phosphoramidase activity of hHint1 has been shown to be necessary for the activation of several preclinical and clinically approved antiviral and anticancer phosphoramidate proTides.[6-9] In addition, Chou and Wagner et al. have demonstrated that lysyl t-RNA synthetase generated lysyl-AMP is a substrate for hHint1 *in vitro*. [10]

Hint1 has been shown to play a role in modulating in N-methyl-D-aspartate (NMDA) receptors activation.[11] The interaction between Hint1 and NMDA receptor has been proposed to mediate the co-association of NMDAR with several G-protein coupled receptors (GPCRs) *in vivo*, including the µ-opioid receptor (MOR).[12, 13] Consistent with this observation, Hint1$^{-/-}$ mice exhibit an increased morphine analgesic response and sensitivity to amphetamine, while reduced nicotine dependence has been observed in self-administration studies.[1-3] In addition, mutations or aberrant expression of hHint1 is been associated with inherited peripheral neuropathy, schizophrenia and bipolar disorders.[14, 15] Nevertheless,

[a] *Department of Medicinal Chemistry University of Minnesota*
Footnotes relating to the title and/or authors should appear here.
Electronic Supplementary Information (ESI) available: [details of any supplementary information available should be included here]. See DOI: 10.1039/x0xx00000x

View Article Online
DOI: 10.1039/C7OB02472J

the identity of the endogenous substrate that presumably is participating in these signaling events has yet to be determined.

Based on the results of our substrate specificity analysis of Hint1,[4] we have designed several competitive inhibitors.[16] Neuropharmacological studies with one of these inhibitors, **3** (TpGc, Supporting Figure S1), revealed that it enhanced morphine analgesia, blocked the development of tolerance and relieved neuropathic pain in mice.[17] We have also demonstrated that Hint1 regulates the function of MOR via its interaction with the NMDA receptor.[17] To facilitate interrogation of the molecular mechanisms governing the cellular function of Hint1, a fluorescent probe that switches on when bound to the protein would be a valuable mechanistic tool. In addition, a fluorescent switch-on probe of the Hint1 active site would aid in the development of high throughput assays for the screening of potential Hint1 inhibitors.

Currently, there are two classes of small molecule based switch-on fluorescent probes: enzymatic activity-dependent probes and enzymatic activity independent probes.[18] In the later case, generally, a solvatochromic fluorophore is attached to the ligand specific to a target protein of interest. Upon binding to the target of interest, the change in the polarity of the environment results in an increase in the fluorescence intensity of the probe.[19] Unfortunately, these probes exhibit high background fluorescence and hence a low ratio of signal to background fluorescence is observed. Herein we report the first fluorescent reporter ligands for hHint1 with switchable properties guided by the principle used in the design of DNA or aptamer-based molecular beacons.[20] Upon binding to hHint1, these switchable probes undergo a conformational change resulting in the quencher becoming less hybridized with the fluorophore and thus exhibiting and increased fluorescence intensity. In the current work, we demonstrate the utility of such probes in performing hHint1-ligand dissociation studies and the selective detection of hHint1 *in vitro*.

Result and Discussion

Design and synthesis of intramolecularly quenched fluorescent nucleotidomimetic probes for hHint1

We envisioned the following two important criteria for the successful development of switch-on fluorescent probes for hHint1: a) the probe should exhibit selective binding affinity for hHint1 and b) there should be a substantial difference in the fluorescence property of the free and the bound probe. One of the characteristic features of hHint1 is its nucleoside-binding motif, which exhibits a preference for binding purine over pyrimidine nucleoside monophosphates. Hence, we selected the fluorescent non-natural nucleosides, 1, N6-ethenoadenosine (EtAd, $ex_{\lambda max}$ 278, $em_{\lambda max}$ 410 nm) (**7**) and thG ($ex_{\lambda max}$ 331, $em_{\lambda max}$ 450 nm), (**8**) to incorporate into the design of our fluorescent probes (Supporting Figure S2).[21, 22]

The selection of EtAd and dGth was based on their high quantum yields (Ø = 0.56 for EtAd and Ø = 0.34 for thG) and long fluorescent lifetimes (~ 20-25 ns) in aqueous buffers. The guanosine mimic, thG, has an additional advantage since it's excitation and emission maxima are at higher wavelengths compared to EtAd (Supporting Figure S2B) To address the second criteria, we decided to incorporate an indolyl group as a fluorescent quencher. A wide variety of chemical moieties can act as a quencher of fluorescence, For example tryptophan is known to induce quenching of certain dyes and fluorophores over relatively short distances via photon-induced electron transfer (PET).[23] Attachment of an indole side chain using a water-soluble acyl-sulfamate linker to the fluorophore nucleoside nearby resulting in quenching of the fluorescence (Figure 1A). We therefore chose to prepare and investigate the fluorescence properties of 5'-indole-3-propionic acid ribose 1, N6-ethenoadenosine sulfamate (7) and 5'-indole-3-propionic acid ribose-2-aminothieno[3,4-d]pyrimidin-4(3H)-one sulfamate **(8)** (Figure 1C).

Compound **7** has been recently reported as a sub-micromolar (K_d = 0.23 µM) inhibitor of hHint1 and was prepared as previously described.[16] The synthesis of compound **8** began with the preparation of 2-Aminothieno[3,4-d]pyrimidine G mimic nucleoside (thG) as reported by Shin et. al[21] with minor modifications (see supplemental information for details). Next, we carried out the acetonide protection of the 2´, 3´- hydroxyl of the ribose sugar of thG, followed by sulfomylation of the 5'-hydroxyl with sulfamoyl chloride to yield 6 (Scheme 1). Coupling of **6** with the activated NHS-ester of an indole-3-propionic acid (**22**) in the presence of DBU and subsequent removal of the acetonide group with aqueous TFA generated **8** in 60 % overall yield. When compared to the parent nucleosides, EtAd and thG, the quantum yields of compounds **7** and

View Article Online
DOI: 10.1039/C7OB02472J

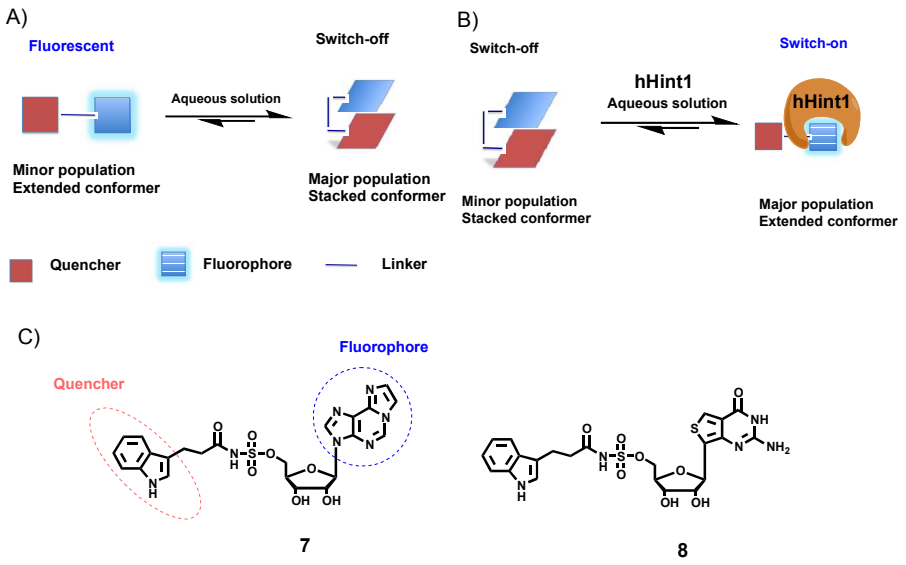

Figure 1. A) Concept of the designed intramolecularly quenched probes for hHint1 B) Upon incubation with hHint1, the probe hybridizes with the complementary active site, resulting in the extended conformer and hence regain in the fluorescence C) Chemical structures of the designed intramolecular quenched probes **7** and **8**. Circled in red is a quencher (indole ring) and blue is the fluorescentnucleobase

8 exhibited a 50- and 19- fold decrease, respectively (Table 1). Studies also revealed a 4- to 5- fold reduction in the fluorescence lifetime of **7** and **8** when compared to the parent nucleosides (Table 1, Supporting Figure S3). Based on the decrease in the fluorescence intensity and lifetime of the fluorophore, we estimate that in an aqueous solution, 89 % and 77% of the population of **7** and **8**, respectively, exists in a stacked conformation (Table 1). The decrease in the average lifetime also indicates that both probes continuously undergo end-to-end dynamic collisional quenching.

Scheme 1[a]

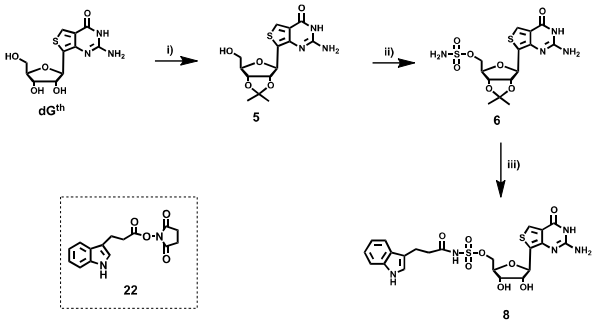

aReagents and conditions: i) perchloric acid and acetone 2 h, ii) NH_2SO_2Cl, DMA, 85%; iii) 22, DBU, DMF 55%; iv) 80 % aq. TFA quant

The unimolecular rate constant (kq) for this process was calculated to be 1.7 x 10^8 per second for both **7** and **8**. Thus, both probes undergo static and dynamic quenching.[24]

Both probes exhibit switch-on fluorescence properties upon incubation with hHint1 in an aqueous solution

Since a stacked conformation for **7** and **8** would result in the quenching of the fluorescence, we reasoned that binding of the probes to hHint1 would lead to decreased end-to-end collision and an increase in the observed fluorescence (Figure 1B). Such phenomenon of fluorescence/FRET behavior has been previously observed upon binding of the cofactor NADH to human 17-B-dehydrogenase complex, but has not been exploited in the design of an inhibitor for a target protein.[25] As expected, an increase in fluorescence intensity was observed upon incubation of these probes in the presence of hHint1 (Figure 2A). Titration of these probes with an increasing amount of hHint1 yielded a fluorescence intensity curve consistent with active site binding in an extended conformation (Figure 2B). Our observation is supported by X-ray co-crystal studies of **7** bound to hHint1.[16]

View Article Online
DOI: 10.1039/C7OB02472J

Recently it was reported that different keto-amino tautomers of the exocyclic amine in the fluorescent thG nucleoside exist in aqueous solution with each possessing a distinct spectral property.[26] Mixtures of the tautomers was found to result in broad emission spectra in aqueous solutions with each tautomer either blue or red-shifted relatively along a narrow emission profile and characterized by a high photostability. The emission profile of our bound probe resembles the red shifted tautomer indicating that binding of the protein is stabilizing a preferred nucleoside tautomer.

Upon inspection of the X-ray crystal structure of **7** bound to Hint1,[16] it can be estimated that the exocyclic amine in guanosine could participate in a hydrogen bonding interaction with backbone carbonyl of His-42, which might result in the stabilization of one tautomer in the bound state. The probes **7** and **8** exhibited a linear increase in the intensity of the emission signal in the absence of proteins, corresponding to EtAd and thG auto or background fluorescence. (Supporting Figure S4). Fitting the observed data with a one site-binding model provided dissociation constant for **7** of 0.121 ± 0.02 µM and **8**, 2.2 ± 0.36 µM. (Figure 2)

The affinity of **7** is in agreement with the previously reported dissociation constant of 0.23 µM obtained by isothermal titration calorimetry (ITC).[16] The dissociation constant of **8** was found to be four-fold lower than the recently reported guanosine analog of **8** by Shah and Wagner et al.[16] This result indicate that the replacement of nitrogen's in the purine ring and the incorporation of a sulfur atom at C8 position results in decreased binding affinity for hHint1.

Utility of switch-on probes in hHint1-ligand binding analysis

Since probes **7** and **8** occupy the active site of hHint1, monitoring their displacement by non-fluorescent ligands would allow us to determine the dissociation constants of the ligands. As can be seen in Figure 3, titration of the hHint1-**7** or **8** complex with the inhibitors Bio-AMS or TpGc yielded a dose-dependent decrease in fluorescence. IC_{50} values obtained from the plot of the % decrease in fluorescence intensity vs. log dose response curve were then converted using the Cheng-Prusoff equation to provide the inhibition constant (K_i) values. The values for both the inhibitors were found to be very similar to the previously reported

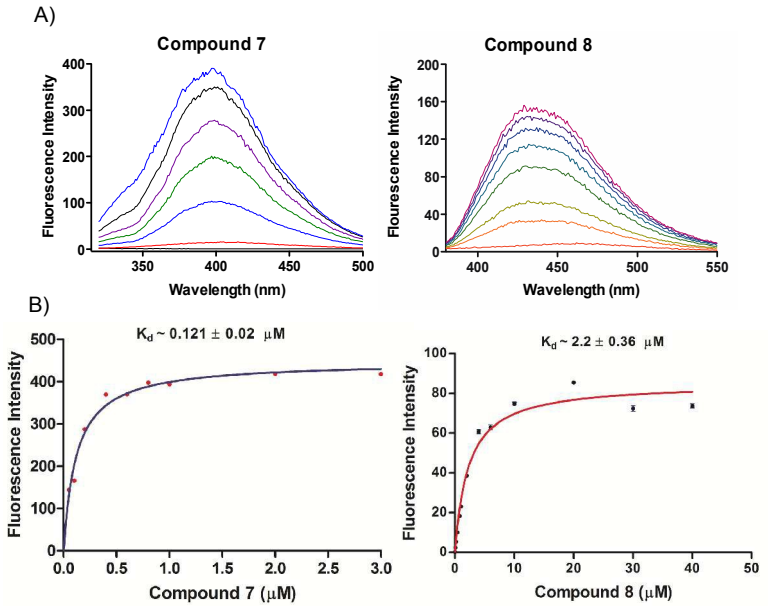

Figure 2. A) Fluorescent spectra changes of compound **7** and **8** (3 µM) upon addition of hHint1 (0.5-6 µM) (λ_{ex}= 278 nm for **7** and 330 nm for **8**) in an aqueous assay buffer with slit width of 5 nm for both excitation and emission. B) Specific binding of probes to hHint1 (0.25 or 1 µM) observed with increasing concentration of ligands. The total increase in the fluorescence (λ_{ex}= 278 nm for **7**, λ_{em}= 410 slit 10 and 330 nm for **8**, λ_{em}= 453 slit 5) was subtracted from the background intensity and plotted against the concentration of the respective compounds. Data points represent three measurements including the standard deviations.

Table 1: Photophysical properties for the fluorescent nucleoside analogues used in the current study

View Article Online
DOI: 10.1039/C7OB02472J

Compound	Quantum yield (Ø)	Lifetime τ (ns)	Extended conformer γ (%)	Stacked conformer 1- γ (%)	k_q (1/s)
EtAd	0.56	25	-	-	-
dGth	0.34	20	-	-	-
7	0.011	4.7	10.8	89.2	1.7×10^8
8	0.018	4.5	23.0	77	1.7×10^8

dissociation constant values of 0.32 and 3.65 μM for Bio-AMS and TrpGc, respectively, via ITC.[16] In similar fashion, the values of the inhibition constants for the nucleoside monophosphates (NMPs) to hHint1 ranged from 20-40 μM with a rank order of GMP≈AMP>CMP>UMP (Table 2).

We next sought to evaluate whether the probes could be used to determine the binding affinity of nucleoside phosphoramidate substrates of hHint1. Instead of the catalytically active enzyme, we employed the catalytically inactive mutant of hHint1, H112A, in which the nucleophilic imidazole was replaced with an alanine residue.[10] As observed for the wild-type enzyme, incubation of hHint1_H112A mutant with **8** resulted in an increase in fluorescence intensity. Interestingly, the hHint1_H112A mutant exhibited a moderate gain (~4 fold) in the binding affinity for **8** compared to the wild-type enzyme (Figure 3B, Table 2). When the hHint1-**8** complex was then titrated with variable concentrations of the hHint1 substrate, TpAd, a dose-dependent decrease in fluorescence was observed corresponding to a dissociation constant of 0.5 ± 0.01 □M (Figure 3B, Table 2).

Our fluorescent probes allow for a rapid mix and measurement of fluorescence for a displacement assay for hHint1. The assay circumvents high concentration of proteins required for the recently reported ITC studies with hHint1 inhibitors. Compound **8** and its cognate fluorescent nucleoside displays properties that make them suitable for the development of a high-throughput-screening (HTS) assay in the identification of new nucleoside or non-nucleoside inhibitors of hHint1. One of the significant limitations that commonly arise in fluorescent-based high throughput assays is the interference from the library compounds that are fluorescent, resulting in false negative or positive hits.[27] Typically, fluorescent compounds in the screening library have a fluorescence lifetime of less than 5 ns. Hence, the use of fluorescence lifetime as the readout parameters for HTS has been shown to increase the robustness against artifacts and compound related interferences.[28, 29] Both our probes exhibit a remarkable change in their fluorescence lifetime (4-5 fold) when unquenched or bound to hHint1. This exceptionally long lifetime (20-25 ns) would offer a robust assay with a high quality primary screening data.

A fluorescent switch-on FRET probe of the active site of hHint1

One of the key motivations in the development of 8 was the realization that the maximum excitation wavelength of thG (ex_{max} = 330-360 nm) overlaps with the fluorescence emission maxima wavelength for tryptophan (em_{max} = 340 nm). The critical Föster resonance distance (R_0) between tryptophan and the fluorescent nucleoside (thG) has been reported to be 22 Å.[30] Inspection of the x-ray crystal structure revealed the presence of a single tryptophan residue (W123) located in the active site that is 13 Å away from the nucleobase-binding pocket (S1) (Figure 4A).

View Article Online
DOI: 10.1039/C7OB02472J

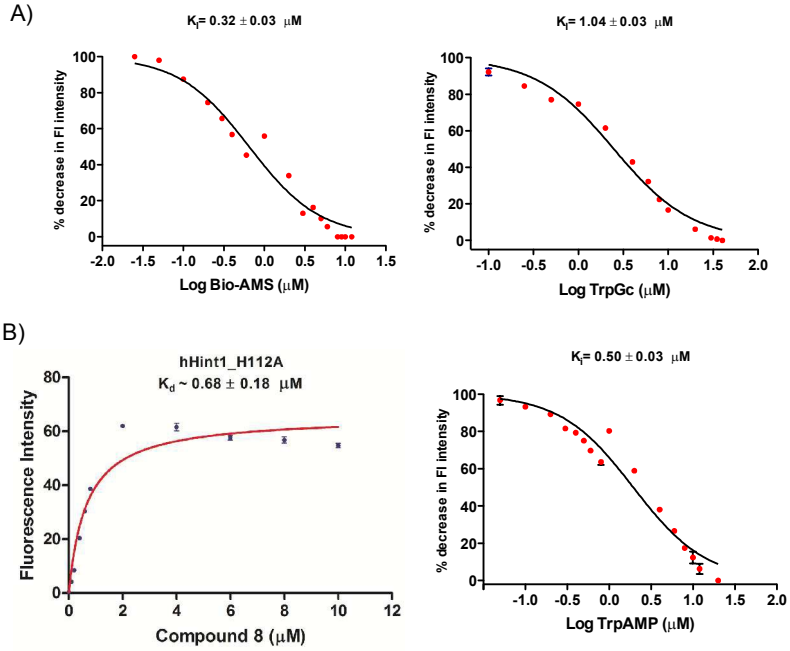

Figure 3. A) Competitive displacement studies (Left) Titration of Bio-AMS (0.025-12 μM) with hHint1 (0.25 μM) incubated with 0.4 μM of compound **7**. (Right) Titration of compound **3** (TrpGc, 1-40 μM) with hHint1 (1.0 μM) incubated with 12 μM M of compound **8**. B) (Left) Specific binding of compound **8** to hHint1_H112A (0.5) observed with increasing concentration of the ligand. The total increase in the fluorescence (λ_{ex}= 330 nm and λ_{em}= 453 nm, slit 5) was plotted against the concentration of the compound **8**. Data points represent three measurements including the standard deviations. (Right) Titration of Hint1 substrate (TrpAMP, 0.025-12 μM) with hHint1_H112A (0.25 μM) incubated with 2.0 μM of compound **8**. One site-binding model was used to fit the displacement curves. Data points represent three measurements, including the standard deviations.

Table 2: hHint1-ligand binding constants calculated using fluorescence displacement studies with switch-on probes.

Ligand	Wild type hHint1		hHint1_H112A	
	IC_{50} (μM)	K_i (μM)	IC_{50} (μM)	K_i (μM)
Bio-AMS[a]	1.77 ± 0.05	0.32 ± 0.03	-	-
3 (TrpGc)[b]	6.71 ± 0.04	1.04 ± 0.03	-	-
AMP[b]	141.9 ± 1.8	22.1 ± 2.1	-	-
GMP[b]	153.99 ± 2.0	23.9 ± 1.9	-	-
UMP[b]	246.82 ± 2.8	38.3 ± 2.3	-	-
CMP[b]	219.95 ± 2.4	34.1 ± 2.4	-	-
2 (TrpAMP)[b]	-	-	1.94 ± 0.05	0.50 ± 0.03

View Article Online
DOI: 10.1039/C7OB02472J

Journal Name

ARTICLE

Such proximity provides an opportunity for the development of a fluorescence resonance energy transfer (FRET) based switch-on probe for hHint1. FRET was verified by measuring the fluorescence emission spectra of hHint1 alone and in the presence of compound **8** (Figure 4A). Upon incubation with an excess amount of hHint1 and excitation at 280 nm; the emission at 360 nm was decreased with an increase in emission signal intensity at 450 nm. This observation is in agreement with those typically seen with FRET pairing molecules. Since the structure of **8** incorporates an indole moiety, one might expect FRET from not only W123 but also from the intramolecular indole side chain. Distinguishing between the two overlaps would be difficult. Hence, we synthesized an analog of **9**, with a biotin instead of the indole side chain. Thermodynamic binding analysis using ITC indicated that **9** binds hHint1 with a dissociation constant of 6.2 ± 0.34 µM (Figure S5 and Table S2). Upon incubation, with hHint1 compound **9** exhibited an increase in emission intensity at 450 nm. (Figure 4B). This result confirms FRET pairing of our probes **8** and **9** with the tryptophan in the active site of hHint1. Our attempts to abolish FRET with a W123A mutation led to the loss of dimerization of hHint1 (data not shown). Mutations associated with a loss in dimerization of hHint1 have been reported to decrease its substrate specificity and Michaelis-Menten constant for the substrates.[31] Hence, we did not observed fluorescence unquenching of compound **8** in the presence of hHint1_W123A mutant (data not shown).

Selectivity of switch-on fluorescence probes on binding to Hint1.

The human genome encodes for three different isoforms of Hint proteins: hHint1, 2 and 3, while prokaryotes such as Escherichia coli encodes only a single protein with phosphoramidase activity (ecHint). Our kinetic and substrate specificity studies with Hint enzymes have clearly shown differences among these isoforms. Incubation of compound **8** with each hHint1 isoforms resulted in differential amounts of fluorescence unquenching. Among them, hHint1 showed the highest, while both hHint3 and echinT exhibited the lowest amount of fluorescence intensity upon incubation with compound **8** (Figure 5A). A similar pattern was observed for the selectivity of probe **7** (Supporting Figure S6). The difference in the amount of unquenching also manifests the ability of the Hint isoforms to differentially bind acyl-NMP and their potential as in vivo regulators. These results are in agreement with the decrease in the Michaels-Menten constant observed for both hHint3 and echinT when the substrate specificity studies of the isoforms and the hHint1 are compared. Interestingly, among these isoforms, only hHint1 and 2 contains a tryptophan, in the active site but not the others. Consequently, we observed the FRET signal only in the presence of hHint1 and 2 (Figure 5C). The ability of our probes to light up upon binding to hHint1 provides a simple and easy means to evaluate the impact of the perturbations on the protein structure on the acyl-NMP binding. For example, an increase in the binding affinity was clearly evident with the catalytically inactive H112A mutation in hHint1.[31] The relative increase in the fluorescence intensity of **8** upon binding to hHint1 provides an insight into the first step in the formation of the ES complex. The ability of **8** to differentiate between hHint1 and Hint2 despite their high sequence and structural similarity indicates the underlying differences in their ability to form an ES complex. Recently, numerous point mutations in hHint1 were identified from clinical patients and were described to be a leading cause of peripheral neuropathy associated with neuromyotonia.[14, 32] In such scenario, our probes could serve as valuable tools in evaluating the impact of these mutations on the binding of potential substrates and products to hHint1.

Next, we wanted to ask if compound 8 would display similar switch-on properties in the presence of other adenylating or nucleoside binding proteins. We chose an aminoacyl t-RNA synthetase (lysRs) as a representative example and dihydrofolate reductase (DHFR) for its ability to bind a nucleotide-based cofactor NADPH. We also used an aminopeptidase protein trypsin in the study. We monitored the increase in the fluorescence intensity of Compound **8** (λ_{ex} = 330 nm, λ_{em} = 450 nm) in the presence of both proteins. Incubation of these proteins with Compound **8** yielded little or no increase in the

View Article Online
DOI: 10.1039/C7OB02472J

fluorescence intensity (Figure 5A). Furthermore, incubation of 8 with the lysate of Escherichia coli (total protein 1 mg) yielded little or no increase in the fluorescence intensity. However, incubation of **8** with *E.coli* lysate (total protein concentration 1 mg/ml) obtained from cells transformed with the hHint1 expression plasmid (IPTG induction 1.5 h) resulted in a significant increase in the fluorescence intensity (Figure 5B). Together, these results demonstrate the ability of Hint1 to bind selectively and switch-on the fluorescence of **8**.

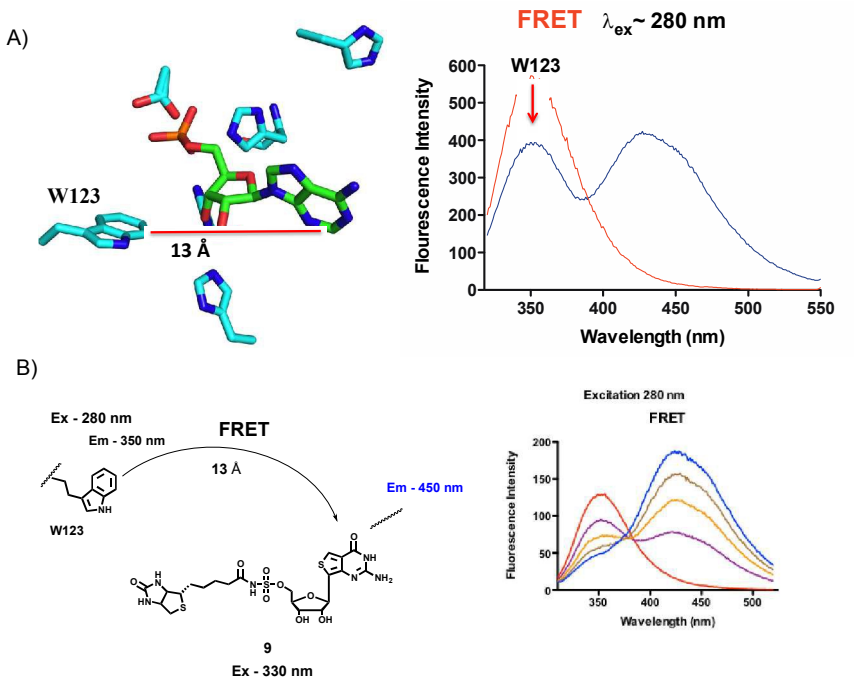

Figure 4. A) (Left) X-ray crystal structure analysis of AMP bound to hHint1 (pdb: 3TW2) to measure the distance between W123 and the nucleobase for FRET pairing (dotted line 13Å). (Right) FRET signal measurement upon incubating 8 µM of hHint1 alone (red) or in the presence of **8** (2 µM) (blue, λ_{ex}= 280 nm for **8**, slit 5) in an aqueous assay buffer. The decrease in the emission intensity (λ_{em}= 360 nm for tryptophan, slit 5) of the protein was observed upon incubation with compound **8**. B) Chemical structure of compound **9** (analogue of 8 without indole side chain) bound which is proposed to FRET pair (dotted line 13Å) with W123 in hHint1. (Right) FRET signal measurement upon incubating hHint1 (1 µM) alone (red) or in the presence of increasing concentration of compound **9** (1.0-4.0 µM) (blue, λ_{ex}= 280 nm, slit 5) in an aqueous assay buffer.

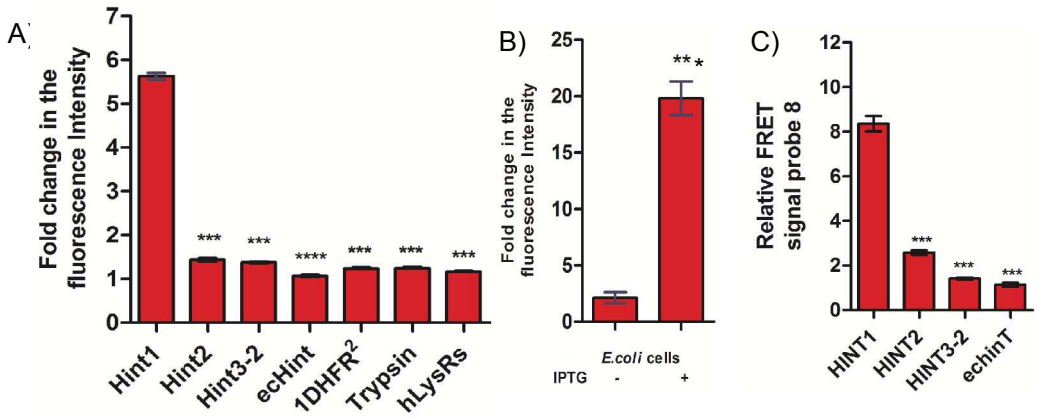

View Article Online
DOI: 10.1039/C7OB02472J

Figure 5. Selectivity test of compound **8** with other proteins: Compound **8** (12 μM) was tested with A) 1 μM of Hint isoforms and three other nucleoside/nucleotide binding proteins or B) *E.coli* lysate (1 mg/ml) without/with hHint1. C) Comparison of signal from FRET pairing of compound 8 with tryptophan in the active site of Hint1 or 2 to other Hint proteins that lacks such tryptophan: Compound **8** (12 μM) was tested with 1 μM of Hint isoform proteins. The observed signal in Hint3-2 and echinT is resulting from the background fluorescence of the unbound probe and hasn't been normalized to that. Student t-test perform on the values indicate, **** p-values < 0.0001, *** p-values ≥ 0.0001

Conclusion:

In conclusion, we have developed a novel fluorescent/FRET probes with switch on properties for selective detection of hHint1. The probes would serve a valuable tool for the future discovery of inhibitors and substrates, as well as aid in studies of the conformation dynamics and molecular recognition of ligands by hHint1.

Acknowledgements

We thank Dr. Kurt J. Peterson at the fluorescence innovations and Dr. Ji Li at the biophysical and spectroscopy facilities at University of Minnesota for help with the fluorescence lifetime studies and helpful discussions. We would also like to thank Dr. Courtney Aldrich lab for providing NHS-ester of Biotin to synthesize compound **9**.

Materials and Methods

Fluorescence Spectroscopy: hHint1-Ligand binding and displacement studies

All fluorescence measurements were performed in an aqueous assay buffer (20 mM Tris, 150 mM NaCl pH 7.4). All fluorescence measurements were performed in a 1 cm four sided, 2 ml quartz cuvette. The total sample of 600-μl solution including the protein and ligand was used in the cuvettes to perform fluorescence measurements. All the readings were recorded at room temperature. The excitation and emission wavelengths and the slit width are described in the legends of the respective figures. The excitation wavelength for dGth and **8** was 330 nm and the emission spectral scan was recorded from 360-530 nm. The excitation wavelength for EtAd and **7** was 280 nm, and the emission spectral scan was recorded from 320-530 nm. In the case of FRET measurement, the excitation wavelength for **8** was done at 280 nm, and emission spectra were recorded from 320-520 nm.

For hHint1-ligand binding studies hHint1 was incubated with successive increase in the concentration of **7** (0.05 -3 μM) or **8** (0.25-40 μM). The mixture was incubated for 30 s before the excitation and following with emission spectral intensity recording at 410 nm and 450 nm. The increase in the fluorescence intensity upon successive increase of the ligand concentration was subtracted from the blank measurement. A blank was recorded in the presence of just the ligand and no protein to yield a linear curve. The resulting sigmoidal dose response curve was plotted in the graph pad prism and fitted using one site-binding model to yield the dissociation constant (K_d) values.

For hHint1-ligand displacement studies hHint1 was incubated with either **7** or **8** at saturating concentrations. The mixture was incubated for 60 s before the addition of the desired ligand for the displacement of the fluorescence. The excitation and emission intensity was recorded. The decrease in the fluorescence intensity upon successive addition of the ligand was normalized to the blank and the resulting dose response curve was plotted in the graph pad prism. The dose response curve was fitted with one site-binding model to yield the IC_{50} values. The values were then converted to the inhibitory constant (K_i) values using Cheng-Prusoff equation.

Fluorescence Spectroscopy: Quantum yield, Fluorescence lifetime and Quenching studies

All the fluorescence and absorbance measurement was performed in the assay buffer. All the readings were recorded at the room temperature. The UV visible measurements were performed in the cary eclipse UV spectrophotometer. 5 nm slit width was used for all the measurements.

View Article Online
DOI: 10.1039/C7OB02472J

Quantum yields ($Ø_F$) for the dGth, nucleoside analogs **7** and **8** were calculated using the following equation.

$$Ø_{F(x)} = (A_s/A_x)(F_x/F_s)(n_x/n_s)^2 Ø_{F(s)}$$

Where s is the standard, x is the nucleoside, A is the absorbance at the excitation wavelength, F is the area under the emission curve, n is the refractive index of the solvent and $Ø_F$ is the quantum yield. The standard compound used in the study was EtAd and its reported quantum yield (0.56). The excitation wavelength of 280 nm for **7** and 330 nm for dGth and **8** was used in the calculation of the quantum yields.

Time resolved fluorescence spectroscopy or fluorescence decay curve measurements were recorded using time correlated single photon count (TCSPC). Samples (1 μM ligands) were excited with tunable dye laser range of 280-305 nm (instrument MatrixUV scientific) with excitation wavelength set at 305 nm for EtAd and **7**. A subnanosecond pulse diode laser 355 ± 5 nm was used for dGth and **8**. Emission was selected using a band pass filter (405 ± 5 nm and 430 ± 5 nm). To avoid anisotropy effects, emission polarizer was set at the magic angle (54.7°) during lifetime measurements. The instruments response function was acquired on the sample containing assay buffer using scattered excitation light detected with emission light polarizer set to vertical (0°) but without an emission filter. The PMT voltage for the emission detection was set to 600 V. The details on the instrument set up is described elsewhere. Fluorescent lifetime decay curves were analyzed using multiexponential decay simulation and nonlinear least square minimization. The observed waveform was fit by the decay simulation which had been iteratively convolved with the measured instrument response function (IRF) using fargo fit analysis software.[33, 34]

Based on the quantum yields and fluorescence lifetime studies, the fraction of population of **7** and **8** in stacked conformation resulting in the static quenching was calculated using equation,

$$□ = (F/F_0)\ (□/□_0)$$

Where □ is the fraction of population in open conformer, 1- □ gives population in closed conformer. F and F_0 is the fluorescence in the presence and absence of the quencher. Parent nucleoside served as control for the absence of an intermolecular quencher. □ and $□_0$ is the fluorescence lifetime in the presence and absence of the quencher. The ratio of □/ $□_0$ gave the fraction of the population under dynamic quenching. The unimolecular rate constant (k_q) for the dynamic intramolecular quenching was calculated using equation,

$$(□/□_0) = 1 + k_q(□_0)$$

$$k_q = 1/□ - 1/□_0$$

Synthesis of the dGth nucleoside and other nucleoside acyl-sulfamates:

The detail information on the synthesis of probes is described in the supplemental information.

References

1. W. Guang, H. Wang, T. Su, I. B. Weinstein and J. B. Wang, *Mol Pharmacol*, 2004, **66**, 1285-1292.
2. E. Barbier, A. Zapata, E. Oh, Q. Liu, F. Zhu, A. Undie, T. Shippenberg and J. B. Wang, *Neuropsychopharmacology*, 2007, **32**, 1774-1782.
3. K. J. Jackson, J. B. Wang, E. Barbier, M. I. Damaj and X. Chen, *Neurosci Lett*, 2013, **550**, 129-133.
4. T. F. Chou, J. Baraniak, R. Kaczmarek, X. Zhou, J. Cheng, B. Ghosh and C. R. Wagner, *Mol Pharm*, 2007, **4**, 208-217.
5. T. F. Chou, I. B. Tikh, B. A. Horta, B. Ghosh, R. B. De Alencastro and C. R. Wagner, *J Biol Chem*, 2007, **282**, 15137-15147.
6. E. Murakami, T. Tolstykh, H. Bao, C. Niu, H. M. Steuer, D. Bao, W. Chang, C. Espiritu, S. Bansal, A. M. Lam, M. J. Otto, M. J. Sofia and P. A. Furman, *J Biol Chem*, 2010, **285**, 34337-34347.
7. D. P. Drontle and C. R. Wagner, *Mini Rev Med Chem*, 2004, **4**, 409-419.
8. S. Li, Y. Jia, B. Jacobson, J. McCauley, R. Kratzke, P. B. Bitterman and C. R. Wagner, *Mol Pharm*, 2013, **10**, 523-531.
9. T. W. Abraham, T. I. Kalman, E. J. McIntee and C. R. Wagner, *J Med Chem*, 1996, **39**, 4569-4575.
10. T. F. Chou and C. R. Wagner, *J Biol Chem*, 2007, **282**, 4719-4727.
11. M. Rodríguez-Muñoz, P. Sánchez-Blázquez, A. Vicente-Sánchez, E. Berrocoso and J. Garzón, *Neuropsychopharmacology*, 2012, **37**, 338-349.
12. M. Rodríguez-Muñoz, P. Sánchez-Blázquez, A. Vicente-Sánchez, C. Bailón, B. Martín-Aznar and J. Garzón, *Cell Mol Life Sci*, 2011, **68**, 2933-2949.
13. J. Garzón, M. Rodríguez-Muñoz and P. Sánchez-Blázquez, *Curr Drug Abuse Rev*, 2012, **5**, 199-226.
14. M. Zimoń, J. Baets, L. Almeida-Souza, E. De Vriendt, J. Nikodinovic, Y. Parman, E. Battaloğlu, Z. Matur, V. Guergueltcheva, I. Tournev, M. Auer-Grumbach, P. De Rijk, B. S. Petersen, T. Müller, E. Fransen, P. Van

View Article Online
DOI: 10.1039/C7OB02472J

Damme, W. N. Löscher, N. Barišić, Z. Mitrovic, S. C. Previtali, H. Topaloğlu, G. Bernert, A. Beleza-Meireles, S. Todorovic, D. Savic-Pavicevic, B. Ishpekova, S. Lechner, K. Peeters, T. Ooms, A. F. Hahn, S. Züchner, V. Timmerman, P. Van Dijck, V. M. Rasic, A. R. Janecke, P. De Jonghe and A. Jordanova, *Nat Genet*, 2012, **44**, 1080-1083.
15. J. Varadarajulu, A. Schmitt, P. Falkai, M. Alsaif, C. W. Turck and D. Martins-de-Souza, *Eur Arch Psychiatry Clin Neurosci*, 2012, **262**, 167-172.
16. R. Shah, A. Strom, A. Zhou, K. M. Maize, B. C. Finzel and C. R. Wagner, *ACS Med Chem Lett*, 2016, **7**, 780-784.
17. J. Garzón, R. Herrero-Labrador, M. Rodríguez-Muñoz, R. Shah, A. Vicente-Sánchez, C. R. Wagner and P. Sánchez-Blázquez, *Neuropharmacology*, 2015, **89**, 412-423.
18. H. Kobayashi, M. Ogawa, R. Alford, P. L. Choyke and Y. Urano, *Chem Rev*, 2010, **110**, 2620-2640.
19. Y. D. Zhuang, P. Y. Chiang, C. W. Wang and K. T. Tan, *Angew Chem Int Ed Engl*, 2013, **52**, 8124-8128.
20. K. Wang, Z. Tang, C. J. Yang, Y. Kim, X. Fang, W. Li, Y. Wu, C. D. Medley, Z. Cao, J. Li, P. Colon, H. Lin and W. Tan, *Angew Chem Int Ed Engl*, 2009, **48**, 856-870.
21. D. Shin, R. W. Sinkeldam and Y. Tor, *J Am Chem Soc*, 2011, **133**, 14912-14915.
22. R. D. Spencer, G. Weber, G. L. Tolman, J. R. Barrio and N. J. Leonard, *Eur J Biochem*, 1974, **45**, 425-429.
23. S. E. Mansoor, M. A. Dewitt and D. L. Farrens, *Biochemistry*, 2010, **49**, 9722-9731.
24. J. R. **Lakowicz** *Principles of Fluorescence Spectroscopy*, 3rd edition edn., 2006.
25. B. Li and S. X. Lin, *Eur J Biochem*, 1996, **235**, 180-186.
26. M. Sholokh, R. Improta, M. Mori, R. Sharma, C. Kenfack, D. Shin, K. Voltz, R. H. Stote, O. A. Zaporozhets, M. Botta, Y. Tor and Y. Mély, *Angew Chem Int Ed Engl*, 2016, **55**, 7974-7978.
27. A. Simeonov, A. Jadhav, C. J. Thomas, Y. Wang, R. Huang, N. T. Southall, P. Shinn, J. Smith, C. P. Austin, D. S. Auld and J. Inglese, *J Med Chem*, 2008, **51**, 2363-2371.
28. S. Pritz, K. Doering, J. Woelcke and U. Hassiepen, *Expert Opin Drug Discov*, 2011, **6**, 663-670.
29. K. J. Petersen, K. C. Peterson, J. M. Muretta, S. E. Higgins, G. D. Gillispie and D. D. Thomas, *Rev Sci Instrum*, 2014, **85**, 113101.
30. Y. Xie, T. Maxson and Y. Tor, *J Am Chem Soc*, 2010, **132**, 11896-11897.
31. X. Zhou, T. F. Chou, B. E. Aubol, C. J. Park, R. Wolfenden, J. Adams and C. R. Wagner, *Biochemistry*, 2013, **52**, 3588-3600.
32. P. Laššuthová, D. Brožková, M. Krůtová, J. Neupauerová, J. Haberlová, R. Mazanec, N. Dvořáčková, Z. Goldenberg and P. Seeman, *Neurogenetics*, 2015, **16**, 43-54.
33. J. M. Autry, J. E. Rubin, B. Svensson, J. Li and D. D. Thomas, *J Biol Chem*, 2012, **287**, 39070-39082.
34. J. M. Muretta, A. Kyrychenko, A. S. Ladokhin, D. J. Kast, G. D. Gillispie and D. D. Thomas, *Rev Sci Instrum*, 2010, **81**, 103101.

View Article Online
DOI: 10.1039/C7OB02472J